Biochemical Pharmacology, Vol. 58, pp. 1915–1925, 1999.

ISSN 0006-2952/99/$–see front matter
PII S0006-2952(99)00282-8

Molecular Mechanism of the Short-Term Cardiotoxicity Caused by 2′,3′-Dideoxycytidine (ddC): Modulation of Reactive Oxygen Species Levels and ADP-Ribosylation Reactions

Gabriella Skuta, Gabor M. Fischer,* Tamas Janaky,† Zoltan Kele,† Pal Szabo,† Jozsef Tozser‡ and Balazs Sumegi*§*

*Department of Biochemistry, University Medical School, Pecs; †Department of Medical Chemistry, Albert Szent-Gyorgyi Medical University, Szeged; and ‡Department of Biochemistry, University Medical School of Debrecen, Debrecen, Hungary

ABSTRACT. The short-term cardiac side effects of 2′,3′-dideoxycytidine (ddC, zalcitabine) were studied in rats in order to understand the biochemical events contributing to the development of ddC-induced cardiomyopathy. In developing animals, ddC treatment provoked a surprisingly rapid appearance of cardiac malfunctions characterized by prolonged RR, PR, and QT intervals and J point depression. The energy metabolism in the heart was compromised, characterized by a decreased creatine phosphate/creatine ratio (from 2.05 normal value to 0.75) and a decreased free ATP/ADP ratio (from 332 normal value to 121). The activity of respiratory complexes (NADH: cytochrome *c* oxidoreductase and cytochrome oxidase) also decreased significantly. Southern blot and polymerase chain reaction analysis did not show deletions or a decrease in the quantity of mitochondrial DNA (mtDNA) deriving from ddC-treated rat hearts, indicating that under our experimental conditions, ddC-induced heart abnormalities were not the direct consequence of mtDNA-related damage. The ddC treatment of rats significantly increased the formation of reactive oxygen species (ROS) in heart and skeletal muscle as determined by the oxidation of non-fluorescent dihydrorhodamine123 to fluorescent rhodamine123 and the oxidation of cellular proteins determined from protein carbonyl content. An activation of the nuclear poly-(ADP-ribose) polymerase (EC 2.4.2.30) and an increase in the mono-ADP-ribosylation of glucose-regulated protein and desmin were observed in the cardiac tissue from ddC-treated animals. A decrease in the quantity of heat shock protein (HSP)70s was also detected, while the level of HSP25 and HSP60 remained unchanged. Surprisingly, ddC treatment induced a skeletal muscle-specific decrease in the quantity of three proteins, one of which was identified by N-terminal sequencing as myoglobin, and another by tandem mass spectrometer sequencing as triosephosphate isomerase (EC 5.3.1.1). These data show that the short term cardiotoxicity of ddC is partially based on ROS-mediated signalling through poly- and mono-ADP-ribosylation reactions and depression of HSP70 levels, whose processes represent a new mtDNA independent mechanism for ddC-induced cell damage. BIOCHEM PHARMACOL **58**;12:1915–1925, 1999. © 1999 Elsevier Science Inc.

KEY WORDS. cardiomyopathy; myopathy; mitochondrial; HIV–AIDS; ddC; mtDNA; free radical; HSP; gene expression; ADP-ribose; GRP78; desmin; protein transport; folding; signalling; chaperone

Nucleoside analogues (dideoxynucleosides and AZT‖ are considered to be effective against HIV and have been beneficially used in AIDS therapy [1–3]. Even after protease inhibitors were introduced into AIDS therapy, nucleoside analogues have remained potent anti-HIV agents in combined therapy, exerting a synergistic antiviral effect [4, 5]. This effect is based on premature chain termination in the virus reverse transcriptase reaction caused by dideoxynucleotide 5′-triphosphates. However, many reports demonstrated that these drugs have several toxic side effects because of incorrect chain termination during the replication of the host cell DNA [1, 3], with these side effects depending on the time of application. After a short period of time, it is most likely that the proliferating tissues are concerned (haemopoetic and gastrointestinal systems) reflected by anaemia and gastrointestinal disorders [6, 7]. After a long period of application, these drugs inhibited the mitochondrial DNA polymerase gamma [3, 8–12], inhibiting mitochondrial DNA replication and causing depletions of mtDNA [11]. Since 13 components of the respiratory chain are encoded by the mammalian mitochondrial ge-

§ Corresponding author: Dr. Balazs Sumegi, Department of Biochemistry, University Medical School, Szigeti ut 12, H-7624 Pecs, Hungary. Tel./FAX: 36 72 326466; E-mail: sumegib@apacs.pote.hu

‖ *Abbreviations:* AZT, 3′-azido-3′-deoxythimidine, zidovudine; ddC, 2′,3′-dideoxycytidine, zalcitabine; ER, endoplasmic reticulum; GRP, glucose-regulated protein; HSP, heat shock protein; HIV, human immunodeficiency virus; IgG, immunoglobulin G; mtDNA, mitochondrial DNA; PCR, polymerase chain reaction; PARP, poly-(ADP-ribose) polymerase; and ROS, reactive oxygen species.

Received 25 January 1999; accepted 22 June 1999.

nome, mutations in mtDNA cripple the oxidative energy production of the cell, with a consequent decrease in ATP synthesis. Therefore, the development of myopathy, cardiomyopathy, and neuropathy after a long-term application is probably due to damage to mtDNA [12, 13].

DdC inhibits HIV type 1 *in vivo* and is therefore successfully used in AIDS therapy [2, 3, 14]. It is very likely that the 5′-triphosphorylated derivate of ddC produced by the cytoplasmic ddC kinase [15] is responsible for its therapeutic and toxic effects. As the very early toxic effects of ddC on the haemopoetic system [6, 7] and its late toxic effects on the mtDNA [16, 17] have been described by other investigators, we have focused here on the short-time side effects of ddC. We detected heart function abnormalities resembling cardiomyopathy and associated with abnormal energy metabolism. In addition, we observed increased ROS formation and enhanced ADP-ribosylation of several muscle proteins which led us to propose a new mechanism for the short-term cardiotoxicity of ddC.

MATERIALS AND METHODS

Materials

DdC, cytochrome *c*, CoA-SH, NAD, NADH, acrylamide, *N*,*N*′-methylene-bis-acrylamide, Coomassie brillant blue, Tween 20, anti-HSP25, anti-HSP60, and anti-HSP70, anti-desmin, anti-mouse and anti-rabbit IgG alkaline phosphatase, peroxidase-conjugated, 5-bromo-4-chloro-3-indolyl phosphate, and nitroblue tetrazolium were from Sigma Chemical Co. Bacteriophage T4 polynucleotide kinase and restriction enzyme Sac I were from Fermentas, and restriction enzyme Sst I was from GIBCO BRL. [Gamma-^{32}P]ATP and [alpha-^{32}P]ATP were from Isotope Ltd. Antibodies developed in rabbit against cytochrome oxidase and complex I were prepared in our laboratory. Anti-(ADP-ribose) antibody was a gift from Drs. Alexander Burkle and Masano Miwa. All other chemicals were of the highest purity commercially available.

Animals and Treatments

Developing Wistar monophyletic rats (80–100 g) were intraperitoneally injected with ddC (1 and 2 mg/kg/day) for up to 2 weeks. Before, during, and after the treatment, cardiac function was monitored by Schiller AT-6 ECG using needle electrodes according to the routine technique (6 limb leads, Einthoven I, II, III and Goldberger aVR, aVL, aVF). Heart frequency, PR, QT intervals, T waves, and J point values were detected with standard methods [18]. After finishing ddC treatment, we waited for 3 days until ddC was excreted, in order to eliminate the direct effect of drug toxicity. Then, control and treated rats were anaesthetized with ketamine and seduxen. Heart and skeletal muscles were rapidly freeze-clamped and either stored in liquid nitrogen or processed immediately to metabolic analysis. Long-term storage of the tissues was performed at −70°.

Enzyme Assays

NADH: cytochrome *c* oxidoreductase, cytochrome oxidase, malate dehydrogenase, citrate synthase, lipoamide dehydrogenase, and carnitine acetyltransferase were determined by standard methods as described previously [19, 20].

Enzymatic Analysis

The quick-freeze method was used for collection of tissue samples. One gram tissue was deproteinized in 4% (v/v) perchloric acid containing 10 mM EDTA. After centrifuging (5000 *g* for 5 min), supernatant was decanted and carefully neutralized by the addition of 5 M KOH. Samples were stored overnight at −20°, recentrifuged and creatine and creatine phosphate concentrations were measured by standard enzymatic analysis as described in [21].

Polyacrylamide Gel Electrophoresis

Heart and skeletal muscle samples were homogenized in 20 mM Tris–HCl buffer, pH 7.4 containing 3 mM EDTA, 5 mM betamercaptoethanol and 1% SDS with an Ultra Turrax homogenizer. After the addition of 1% bromphenol blue, samples were boiled for 2 min and clarified by centrifuging (8000 *g* for 2 min). SDS–PAGE was carried out on 12% gel by Laemmli's method [22]. A low molecular weight calibration kit (Pharmacia) was used for estimation of the molecular weight. Gels were stained with Coomassie brillant blue R-250 and destained with solution containing 5% (v/v) acetic acid and 16% (v/v) methanol.

Detection of ROS

ROS detection was performed basically by the same procedure as described in [23, 24]. Hearts from control or ddC-treated animals were removed and freeze-clamped. Heart pieces were homogenized at 4° in 3 mL buffer containing 150 mM KCl, 20 mM Tris, 0.5 mM EDTA, 1 mM $MgCl_2$, 5 mM glucose, and 0.5 mM octanoic acid, pH 7.4. After the addition of 5 μM dihydrorhodamine123, the reaction mixtures were incubated at 37° for 30 min. The reaction was stopped by the addition of an equal amount of ice-cold 70% ethanol which contained 0.1 M HCl and the fluorescent dyes were extracted. The precipitated proteins were removed by centrifuging at 3000 *g* for 15 min. The precipitate was extracted once again, and the unified supernatant aliquots were neutralized with $NaHCO_3$ and centrifuged at 6000 *g*. To correct background fluorescence, samples were incubated under the same conditions but without fluorescent dyes, and 5 μM dihydrorhodamine123 or 5 μM dihydrofluorescein diacetate was given to the tissue only at the end of the incubation period. The fluorescent dye content in the clear supernatants was determined using a Perkin Elmer fluorescent spectroscope at an excitation wavelength of 500 nm and an emission wavelength of 536 nm for rhodamine123.

N-Terminal Sequencing

Proteins separated on 12% SDS–polyacrylamide gels were blotted onto Immobilon-P polyvinylidene difluoride transfer membrane (Millipore Co.) and stained with Coomassie brillant blue R-250. Stained bands were cut out and loaded onto a Knauer Protein Sequencer 910 for N-terminal sequence analysis by Edman degradation. The obtained sequence was compared to the sequences of the Swiss-Prot protein data bank by using the Fasta program.

Protein Identification by Peptide Mass Mapping and Tandem Mass Spectrometry

In-gel digestion of Coomassie-stained protein and extraction of the resulting peptides were carried out according to methods similar to those described in the literature [25]. Briefly, this entailed excising the band of interest, reducing disulfide bonds with dithiothreitol (10 mM dithiothreitol in 0.1 M ammonium bicarbonate buffer, pH = 8.0), alkylating Cys residues with iodoacetamide (55 mM iodoacetamide in 0.1 M ammonium bicarbonate buffer, pH = 8.0), and digesting protein with trypsin (0.1 mg trypsin/mg digested protein in 0.1 M ammonium bicarbonate buffer, pH = 8.0). Proteolytic peptides were dissolved from gel matrix and separated by capillary HPLC. Column eluate was monitored by a UV detector at 210 nm and by a mass spectrometer equipped with an electronspray ion source (Finnigan MAT TSQ-7000). Analyzing molecular weights of peptides formed by tryptic cleavage resulted in the peptide mass map. For tandem mass spectrometric sequence determination, tandem mass spectra of selected digested peptides were acquired. The computer software ProFound (publicly available over the Internet at URL http://prowl.rockefeller.edu/cgi-bin/ProFound) was used to identify proteins in the gel. This program allows the searching of protein or nucleotide sequence databases (SWISS-PROT, PIR, GENPEPT, OWL, or dbEST), using a combination of information from peptide mass map and tandem mass spectra of proteolytic peptides [26].

Western Blot Analysis

The composition of respiratory complexes and HSPs was examined by the Western blot technique. Samples were processed and electrophoresed as described above. For immunoblotting, separated proteins were transferred to nitrocellulose filters. The filters were blocked with 2% low-fat milk in Tris-buffered saline (150 mM NaCl, 20 mM Tris–HCl, pH 7.5) containing 1% polyethylene glycol 6000, and incubated with the first antibody (either anti-HSP25, anti-HSP60, anti-HSP70, or anti-cytochrome oxidase) diluted in the same solution. Nitrocellulose filters were washed three times for 10 min in TBS containing 0.2% Tween 20 and in TBS once more. Adsorbed IgG was detected by incubating the filters with a second antibody (anti-mouse or anti-rabbit IgG alkaline phosphatase conjugate). The labelled proteins were developed with 5-bromo-4-chloro-3-indolyl phosphate and nitroblue tetrazolium as substrates in reaction buffer (200 mM Tris–HCl, 5 mM $MgCl_2$, pH 9.3). Western blot data were analyzed by the Image Tool (Version 1.27) image processing program.

ADP-Ribosylation Assay

Endogenous ADP-ribosylation in heart was essentially determined as described before [24]. Cardiac muscle was homogenized with Ultra-Turrax in 50 mM Tris, pH 7.8 and an equal volume of twice-concentrated Laemmli sample buffer was added. The sample was further homogenized with Potter and centrifuged in an Eppendorf centrifuge. To the supernatant, 1% bromophenol blue was added. In some experiments, the extraction buffer contained 8 M urea, 20 mM Tris, and 4 mM EDTA. For SDS gel electrophoresis, a 10% gel was used. In immunoblotting, anti-ADP-ribose, a mouse monoclonal antibody, was used as a first antibody and peroxidase-labelled anti-mouse IgG as a second antibody. The reaction was visualized by enhanced chemiluminescence.

Immunoaffinity Purification and ADP-Ribosylation of GRP78 and Desmin

DNA-K antibody was coupled to protein A-Sepharose beads and incubated with detergent-solubilized ER proteins at room temperature for 30 min. The gel was washed 3 times with 20 mM Tris–HCl buffer, pH 7.4 containing 150 mM NaCl to remove unbound proteins. The antigen–antibody complex was removed with an equal volume of twice-concentrated Laemmli sample buffer, and used for SDS–PAGE followed by Western blotting with anti-ADP-ribose antibody. Immunopurification of desmin was performed in almost the same way as described for GRP78, except that anti-desmin antibodies were bound to protein A-Sepharose beads and a total cell extract was used for the immunopurification of desmin. The ADP-ribosylation of desmin was detected as described above.

Southern Blot Analysis

Total DNA was prepared from the skeletal muscle of control and ddC-treated animals. DNAs were digested with Sst I or Sac I, and electrophoresed through 1.5% agarose gel, then transferred to nylon membrane (Hybound-N, Amersham) as described in [27]. The mtDNA was prepared from the normal rat liver as described in [28], digested with Sst I, labelled with alpha ^{32}P and used as probe for Southern blotting. The hybridization of blotted DNA and mtDNA probe was performed under the standard conditions using the Sigma kit, and visualized by autoradiogaphy.

TABLE 1. Effect of ddC treatment on cardiac function of developing rats

Treatments	RR (msec)	PR (msec)	QT (msec)	J (mm)
Control	149.0 ± 4	47.2 ± 2.1	61.4 ± 3.0	−0.15 ± 0.04
1-week treatment	156.0 ± 12.0	54.2 ± 3.1	68.2 ± 2.4	−0.92 ± 0.10*
2-week treatment	164.2 ± 6.5	57.0 ± 2.9†	71.0 ± 4.8†	−1.21 ± 0.11*

ECG analysis was performed as described under Materials and Methods. Data represent means ± SEM for 5 animals.
*Values are different from the corresponding values of age-matched control rats at the significance level of $P < 0.001$.
†Values are different from the corresponding values of age-matched control rats at the significance level of $P < 0.01$.

PCR Amplifications

PCR amplification was carried out in a Techne PHC-3 Thermal Cycler. For the amplification of mtDNA deletions, the following primer pairs were used: L 2773 − H 695, L 2773 − H 11120, L 2773 − H 15330, L 11231 − H 695, L 11231 − H 3678, and L 11231 − H 15330. The 50-μL PCR reaction mixture contained 250 ng template DNA, 0.2 mM of each dNTP, 50 mM KCl, 3 mM $MgCl_2$, 10 mM Tris–HCl, pH 9.0, 10 pmol of each primer, and 2 units of Taq DNA polymerase (Pharmacia Biotech). The amplification conditions were as follows: 94° for 5 min, 60° for 30 sec, 72° for 1 min 30 sec in the 1st cycle, followed by 35 cycles of 94° for 30 sec, 60° for 30 sec, and 72° for 1 min 30 sec. The last cycle times were: 94° for 30 sec, 60° for 30 sec, and 72° for 10 min. Ten microlitres of each PCR product was analyzed in horizontal gels of 1.6% agarose with 15 μg ethidium bromide, visualized, and photographed with a UV transilluminator.

End Labelling of 5′ Terminus of DNA

Total DNA was prepared from the skeletal muscle of control and ddC-treated animals by the standard method. The transfer of ^{32}P to the 5′ terminus of DNA was catalyzed by bacteriophage T4 polynucleotide kinase. In the forward reaction, the gamma ^{32}P of [gamma ^{32}P]ATP was transferred to a hydroxyl group created by removal of phosphate from the 5′ terminus of DNA by alkaline phosphatase as described in [27]. After the labelling procedure, DNA was electrophoresed through 1% agarose gel, transferred to nylon membrane (Hybound-N, Amersham) according to a routine method, and studied by autoradiography.

RESULTS

ECG Analysis

ECG was used to follow the changes in heart function of ddC-treated rats. The animals developed a cardiac disturbance with both de- and repolarization deviations. Characteristic ECG differences had already been evident after 1 week of ddC administration and had become more pronounced by the end of the treatment. We observed prolonged PR and QT intervals with otherwise nearly normal heart rates (Table 1). Almost every animal developed a significant J point depression which was most conspicuous in leads I and aVL, corresponding to the main muscle mass of the left ventricle (Table 1). In some cases, arrhythmia was observed, most probably caused by the toxic effect of ddC on sinus and AV nodes (data not shown). Heart function was monitored even after the termination of ddC treatment, and only a slight improvement was observed in the 6-month recovery period. It can be concluded that ddC induced a lasting cardiomyopathy which was not a consequence of the direct inflammatory effect of the drug.

Effect of ddC on Energy Metabolism and Mitochondrial Enzyme Activities

Levels of the metabolites characteristic for heart energy metabolism (creatine, creatine phosphate, ATP, and ADP) were determined in the heart muscle of ddC-treated animals. Significant decreases were detected in ATP and creatine phosphate concentrations as the consequence of 14-day ddC treatment (Table 2). The creatine phosphate/creatine ratio decreased from the normal 2.05 value to 0.75 (Table 2), which corresponded to a decrease in the calculated free ATP/ADP ratio from 332 to 121. These data show that ddC treatment impaired the mitochondrial energy metabolism in the cardiac tissue. To gain insight into the changes in mitochondrial function, we measured the effect of ddC treatment on the activities of mitochondrial respiratory complexes. A drastic reduction in the activities of NADH: cytochrome *c* oxidoreductase and cytochrome oxidase were found (Table 3). Other enzymes studied showed only moderate changes (Table 3). The decrease in enzyme activities suggested a functional defect in oxidative phosphorylation, which is in accordance with

TABLE 2. Effect of ddC treatment on the creatine–creatine phosphate system in rat hearts

	Control	ddC-Treated
	μmol/gram protein	
ATP	23.0 ± 1.8	16.3 ± 1.9*
ADP	4.8 ± 0.5	6.6 ± 0.7
Creatine phosphate	43.3 ± 2.9	19.2 ± 3.1*
Creatine	21.1 ± 1.2	25.7 ± 1.5
Creatine phosphate/creatine ratio	2.05	0.75*
Calculated ATP/ADP ratio	332	121*

Metabolic analysis was performed as described under Materials and Methods. Values represent means ± SEM of four animals.
*Values are different from the corresponding values of age-matched controls at the significance level of $P < 0.01$.

TABLE 3. Comparison of enzyme activities of ddC-treated and control animals

	Skeletal muscle		Heart muscle	
Enzymes	Control	ddC-Treated	Control	ddC-Treated
	U/g wet tissue			
NADH: cytochrome *c* oxidoreductase	6.2 ± 0.4	2.2 ± 0.2*	27.7 ± 2.1	4.4 ± 0.7*
Cytochrome oxidase	56.7 ± 4.1	42.6 ± 3.7†	142.8 ± 9.8	97.9 ± 8.2†
Lipoamide dehydrogenase	8.6 ± 1.0	8.69 ± 0.9	83.7 ± 9.1	65.4 ± 7.2
Citrate synthase	24.7 ± 2.5	15.3 ± 3.6	108 ± 10	101 ± 12
Carnitine acetyltransferase	2.50 ± 0.2	2.9 ± 0.3	6.5 ± 0.6	7.6 ± 0.8
Malate dehydrogenase	459 ± 41	540 ± 60	1263 ± 98	1478 ± 17

Enzyme activity measurements were performed as described under Materials and Methods. Values represent means ± SEM for 4 animals.
*Values are different from the corresponding values of age-matched control values at the significance level of $P < 0.001$.
†Values are different from the corresponding values of age-matched control values at the significance level of $P < 0.01$.

the metabolic data shown in Table 2. The decrease in the activity of mitochondrial enzymes raises the possibility that ddC treatment either affected synthesis, transport, or assembly of respiratory complexes. In an attempt to gather more information on the background of the decreased activities, Complex I and cytochrome oxidase of the ddC-treated animals were studied by the Western blot technique. We could not find significant changes in Complex I (data not shown). The quantity and the polypeptide composition of cytochrome oxidase was also studied, but only minor reductions were seen in the quantity of protein and only slight changes in the polypeptide compositions (data not shown). These data indicated that there was not any general defect in the protein synthesis of mitochondrially or nuclearly encoded polypeptide components of the respiratory complexes.

Effect of ddC on the Quality of DNA of Cardiac and Skeletal Muscle

A possible target of dideoxynucleoside analogues may be the mtDNA, because these anti-HIV drugs, inhibiting mtDNA polymerase gamma, can cause deletions or depletion of mtDNA. Therefore, we searched for mtDNA damage in heart and skeletal muscle of ddC-treated animals by Southern blot analysis. Under our experimental conditions (short-term treatment), no significant deletion or depletion of mtDNA was seen (Fig. 1). Furthermore, we tried to show deletions in mtDNA by PCR analysis using several mitochondrial primer pairs. However, we could not detect deletions in mtDNA in either case under our experimental conditions (data not shown). These data indicate that a 2-week treatment was not sufficiently long to initiate detectable damage in mtDNA, and the observed pathological effects of ddC were not mediated by mtDNA damage. Fragmentation of nuclear DNA is a characteristic of apoptosis, often induced by toxic drugs [29]. Since ddC metabolites can interfere with DNA replication, it is reasonable to assume that ddC may induce apoptotic degradation of nuclear DNA. Using the DNA end labelling method and autoradiography, we investigated whether the ddC induced DNA fragmentation characteristic of apoptosis. Our experiments did not provide any evidence for fragmentation of nuclear DNA, which would indicate apoptosis either in skeletal or cardiac muscle cells (data not shown).

Effect of ddC Treatment on HSP Levels

Malfunction in the transport and assembly of respiratory complexes raises the possibility that the levels of HSP, which are involved in the transport and assembly of the polypeptide components of respiratory complexes, may be

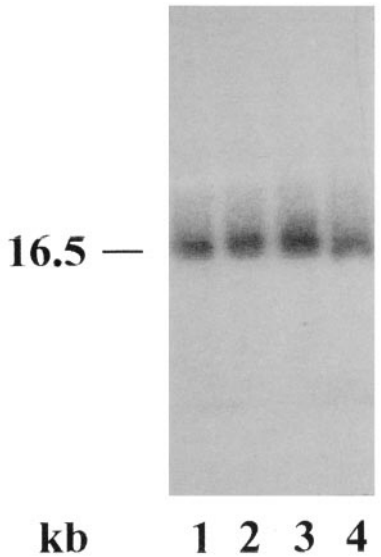

FIG. 1. Effect of ddC treatment on the quality and quantity of mtDNA in cardiac muscle. Southern blot analysis was performed as described under Materials and Methods. Lane 1, DNA from the heart of control animal (4 μg); lanes 2–4, DNAs from the heart of ddC-treated animals (4 μg).

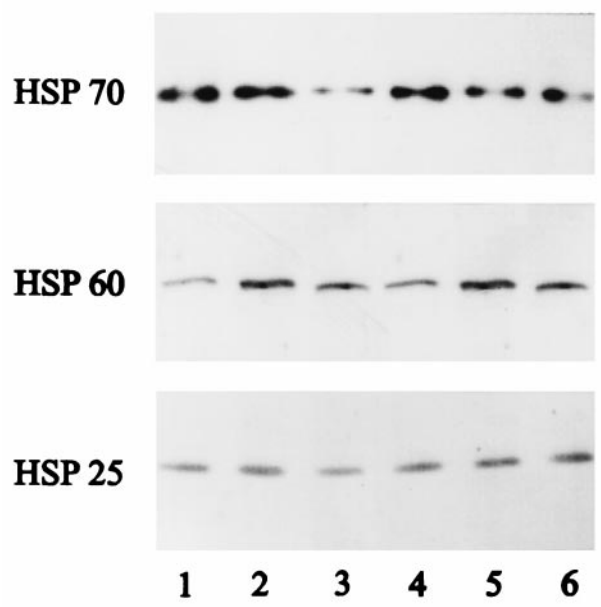

FIG. 2. Effect of ddC treatment on the HSP25, HSP60, and HSP70 levels in heart and skeletal muscles determined by Western blotting. Lane 1, control heart (20 μg protein); lane 2, heart muscle after 6 days of ddC treatment (20 μg protein); lane 3, heart muscle after 14 days of ddC treatment (20 μg protein); lane 4, control skeletal muscle (20 μg protein); lane 5, Skeletal muscle after 6 days of ddC treatment (20 μg protein); lane 6, skeletal muscle after 14 days of ddC treatment (20 μg protein). Experimental conditions are described under Materials and Methods.

affected as a consequence of ddC treatment. The cardiac concentration of HSP25, HSP60, and HSP70 was determined by the immunoblot method, using monoclonal antibodies. Monoclonal anti-HSP25 reacts with the constitutively expressed 25 kD muscle protein. Monoclonal anti-HSP60 is specific for mammalian HSP60, but reacts with both constitutive and inducible HSP60 [30]. Monoclonal anti-HSP70 reacts with both constitutive HSP73 and inducible HSP72 in mammals [31]. Our data indicate that ddC treatment did not change the level of HSP25 and HSP60 either in skeletal or in cardiac muscle during the short-term ddC treatment (Fig. 2). However, a significant reduction was seen in the HSP72 and HSP73 bands both in cardiac and skeletal muscle as a consequence of ddC treatment (Fig. 2, Table 4).

Effect of ddC Treatment on ROS Formation and Protein Oxidation

ROS oxidize dihydrorhodamine123 to fluorescent rhodamine123 [23, 24], providing a method to detect ROS in tissues. The *in vitro* addition of ddC to the reaction mixture did not cause a significant increase in ROS production, indicating that ddC as an organic molecule was not the source of free radicals (data not shown). The short-term ddC treatment induced a large increase in ROS formation, both in the skeletal and cardiac tissues (Table 5). These data indicate that ddC treatment induced slow, unfavourable changes in the heart and skeletal muscle, leading to excess production of ROS. Under *in vivo* conditions, ROS can oxidize proteins, forming reactive aldehyde groups. Therefore, the amount of the protein-bound reactive aldehyde group indicates the level of oxidative damage *in vivo* [32]. In age-matched control rats, the amount of the protein carbonyl group was similar to data previously reported [24]. Two weeks of ddC treatment significantly increased the carbonyl content of the rat heart and skeletal muscle proteins (Table 5) as compared to the age-matched controls.

TABLE 4. Quantitative analysis of the effect of ddC treatment on the HSP25, HSP60, and HSP70 levels in heart and skeletal muscles determined by Western blotting

	HSP25	HSP60	HSP70
	Signal intensities are given in arbitrary units		
Heart muscle			
Control	55 ± 7	93 ± 12	153 ± 11
ddC (7 days)	61 ± 8	127 ± 14	149 ± 12
ddC (14 days)	47 ± 7	108 ± 13	53 ± 10*
Skeletal muscle			
Control	64 ± 8	107 ± 15	150 ± 9
ddC (7 days)	76 ± 9	137 ± 16	106 ± 8†
ddC (14 days)	78 ± 8	125 ± 14	87 ± 10*

Western blot analysis was performed as described under Materials and Methods. Values represent means ± SEM for four Western blot analysis.

*Values are different from the corresponding control values at the significance level of $P < 0.001$.

†Values are different from the corresponding control values at the significance level of $P < 0.01$.

ADP-Ribosylation of Cardiac Proteins

The ADP-ribosylation of intracellular proteins can be affected by several toxic agents [33–35, 24]; therefore, we considered it reasonable to study how the ADP-ribosylation of proteins changes as the consequence of ddC administra-

TABLE 5. Effect of ddC treatment on the formation of reactive oxygen intermediates and oxidative protein modifications in skeletal and cardiac muscle

	Rate of DHR oxidation (in arbitrary units)	Protein carbonyl content (nmol carbonyl/mg protein)
Skeletal muscle		
Control	160.7 ± 2.8	5.24 ± 0.46
ddC-Treated	295.2 ± 8.7*	8.87 ± 0.51†
Cardiac muscle		
Control	318.7 ± 12.4	5.97 ± 0.53
ddC-Treated	613.2 ± 17.1*	11.62 ± 0.67*

ROS determinations and protein carbonyl content analysis were performed as described under Materials and Methods. Values represent means ± SEM for 4 animals. DHR, dihydrorhodamine123.

*Values are different from the corresponding values of age-matched controls at the significance level of $P < 0.001$.

†Value is different from the corresponding values of age-matched controls at the significance level of $P < 0.01$.

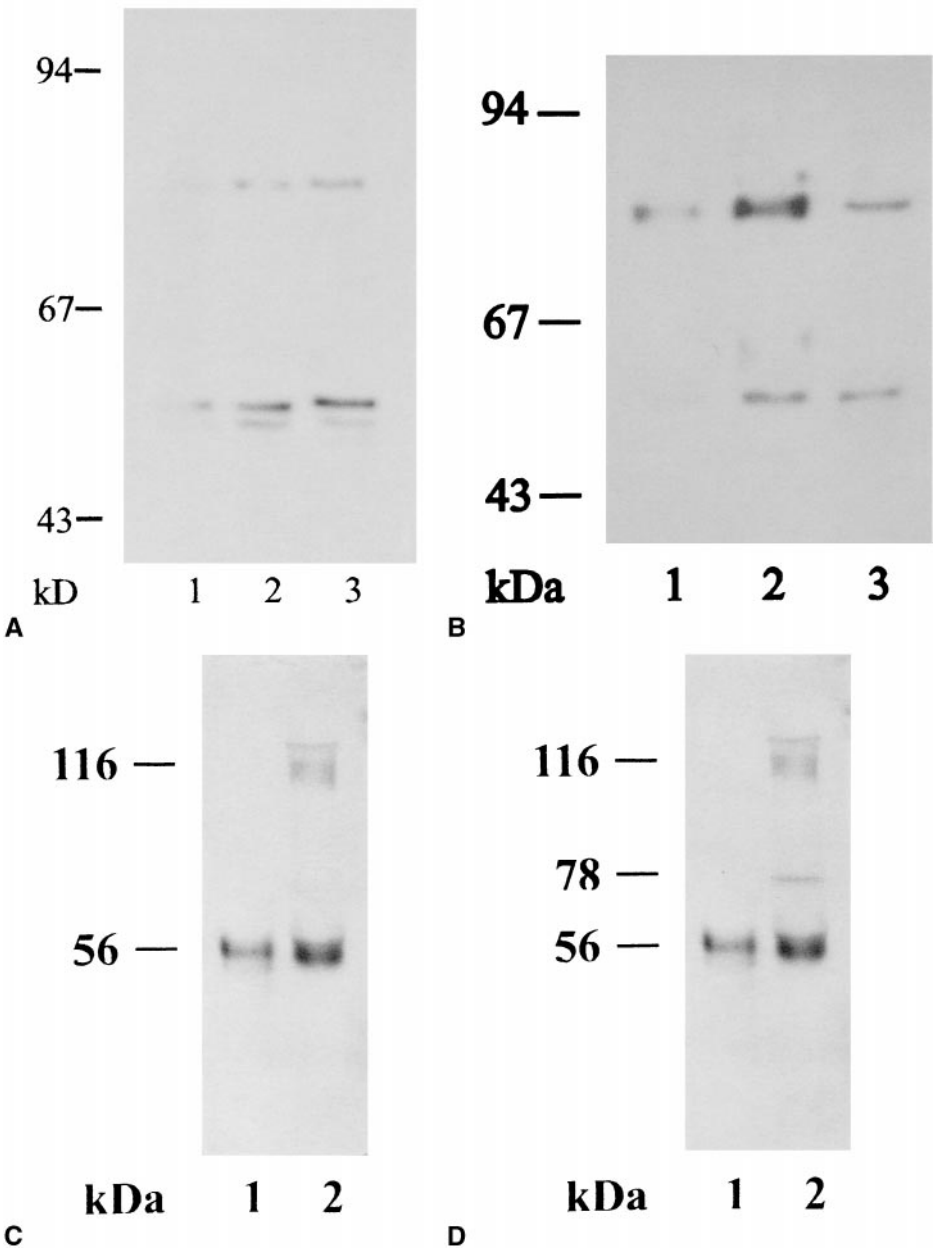

FIG. 3. Effect of ddC treatment on the endogeous ADP-ribosylation of heart proteins. (A) Mono-ADP-ribosylation of 78 and 56 kD proteins. Lane 1; 20 μg protein from control heart muscle; lane 2, 20 μg protein from heart muscle after 7 days of ddC treatment; lane 3, 20 μg protein from heart muscle after 14 days of ddC treatment. (B) Identification of 78 kD protein by immunoprecipitation with anti-GRP78 antibodies and determination of its ADP-ribosylation by Western blotting. Lane 1, immunoprecipitated GRP78 from sarcoplasmic reticulum; lane 2, heart sarcoplasmic reticulum (5 μg protein); lane 3, 20 μg protein from control heart muscle. (C) Identification of 56 kD protein by immunoprecipitation with anti-desmin antibodies and determination of its ADP-ribosylation by Western blotting. Lane 1, immunoprecipitated desmin; lane 2, control heart muscle (20 μg protein). (D) Determination of the self poly-ADP-ribosylasion of PARP. Lane 1, control heart muscle (20 μg protein); lane 2, ddC-treated heart muscle (20 μg protein). Experimental conditions are described under Materials and Methods.

tion. Previous data indicated that the main target proteins of the endogenous mono-ADP-ribosyltransferases in rat heart and muscle tissues are in the regions of 52–56, 78, and above 100 kD [36, 37, 33]. Under our experimental conditions, 78 kD and 56 kD ADP-ribosylated proteins were detectable by Western blot in control hearts, and ddC treatment increased the ADP-ribosylation of these proteins (Fig. 3A). The ADP-ribosylation of skeletal muscle proteins was much less detectable in our system, so did not allow quantitative studies (data not shown). We assumed on the basis of a previous work [38] that the 78 kD ADP-ribosylated protein is the glucose-regulated protein called BIP or GRP78 [38], which belongs to the HSP70 family. To prove this, we immunoprecipitated GRP78 from isolated ER with anti-HSP70 antibodies, and the ADP-ribosylation of the immunoprecipitated protein was detected with antibodies specific for ADP-ribose on Western blots. These data show (Fig. 3B) that 78 kD ADP-ribosylated protein is the GRP78. A similar immunoprecipitation and immunoblot technique was used for the identification of the 56 kD ADP-ribosylated protein. The immunoblot data indicated that the 56 kD ADP-ribosylated protein could be precipitated with anti-desmin antibody (Fig. 3C). From this data, we can conclude that in cardiac muscle, ddC treatment induced the ADP-ribosylation of desmin as well. When the extraction of heart proteins was performed in the presence of 8 M urea, the nuclear PARP (EC 2.4.2.30) was also extracted. Using the Western blot technique as described above, an activation of nuclear PARP was found as a consequence of the ddC treatment (Fig. 3D), which is consistent with the observation that ddC treatment increased ROS production *in vivo* (Table 5).

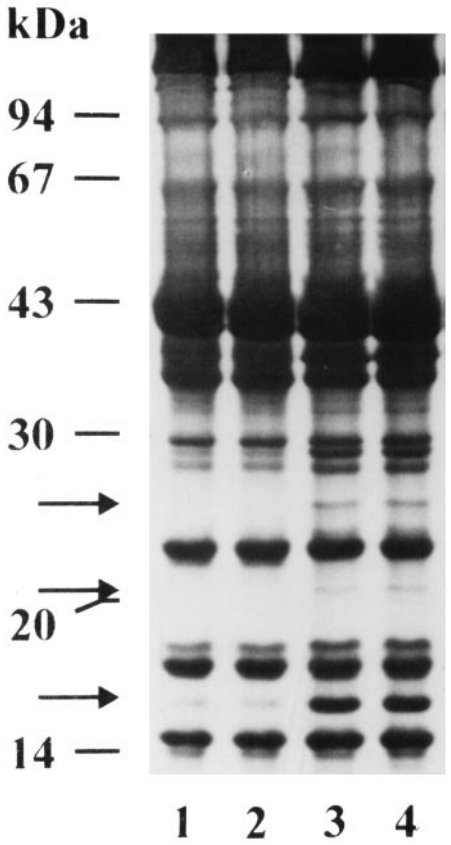

FIG. 4. Comparison of skeletal muscle protein composition in ddC-treated and control animals. SDS-polyacrylamide gel electrophoresis with Comassie brillant blue staining. Lanes 1 and 2, rat skeletal muscles from ddC-treated animals (40 μg protein); lanes 3 and 4, control rat skeletal muscles (40 μg protein). Experimental conditions are described under Materials and Methods.

Identification of Missing Proteins in Muscle by N-Terminal Sequencing and Tandem Mass Spectrometry

The protein composition of heart and skeletal muscles was studied by SDS-gel electrophoresis. By this method, we found some specific differences in the protein composition of skeletal muscle of control and ddC-treated rats while the overall protein composition looked the same (Fig. 4). In the ddC-treated skeletal muscles, three low molecular weight protein bands were missing in the regions of 26 kD, 21 kD, and 16 kD (Fig. 4). In the heart muscle, we could not find a marked difference in the protein composition by this method (data not shown). An attempt to determine the N-terminal sequence of these proteins did not yield results in the cases of 21 and 26 kD molecular mass proteins, probably because their N-terminal was blocked. In the case of the 16 kDa protein, the Edman degradation gave the sequence of GLSDGEWQMVLNDWG. This sequence is 93% homologous to the *N*-terminal sequence of mouse myoglobin (GLSDGEWQLVLN-VWG). Based on the identical molecular masses and the high sequence homology, the 16 kDa protein was very likely rat myoglobin. In-gel tryptic digest of the 26 kD protein band resulted in a peptide mass map with a large number of peaks on the LC–MS chromatogram. We performed a database search based upon the 11 most abundant peptides, using the stringency parameter of ±1 D. The top candidate protein was the triosephosphate isomerase (EC 5.3.1.1) from rat (MW = 26790). Ten of the eleven peptides covered 54% of the sequence of triosephosphate isomerase. To strengthen the prediction of the peptide mass mapping experiment, two of the most intense peptide ions (MW = 1319.5 and MW = 1326.5) were sequenced by tandem mass spectrometry. Interpretation of the fragmentation patterns of these peptides provided two aminoacid sequences (AIADNVKDWCK and IIYGGVTGATCK) which corresponded to the sequences of the 149–159 and 206–218 fragments of triosephosphate isomerase.

DISCUSSION

It is well documented that the anti-HIV drugs (including ddC) which inhibit reverse transcriptase also inhibit the human DNA polymerases, especially the mitochondrial DNA polymerase γ [8, 3, 9]. Therefore, most of the side effects of these drugs were interpreted as the consequence of the inhibition of mitochondrial DNA replication [9, 16]. Recent data suggested that, at least in the case of AZT, the nucleotide analogue has a short-term inhibitory effect on mitochondrial oxidative energy production that cannot be associated with depletion or damage of mtDNA [39]. This inhibitory effect was localized to NADH: citochrome *c* oxidoreductase [40]. Furthermore, there are suggestions that AZT metabolites induce free radical formation in isolated mitochondria [24]. In addition, AZT monophosphate inhibits glycosphingolipid and ganglioside biosynthesis [41].

Much less information is available about the cytotoxicity of ddC and most of its side effects are regarded as the consequence of the inhibition of mtDNA replication [8, 3]. In this study, we investigated the short-term toxic effects of ddC in a rat model. Our data indicated that cardiomyopathy developed (Table 1) before the appearance of any sign of mtDNA depletion or detectable mtDNA damage (Fig. 1). We demonstrated the development of cardiac malfunctions by electrocardiography (ECG) after a short period of treatment with ddC without any sign of defect to the mtDNA (Fig. 1), indicating that the short term cardiotoxicity of ddC developed by a different mechanism. Metabolic studies showed a decreased creatine phosphate level which resulted in a decreased creatine phosphate/creatine ratio (from 2.05 normal value to 0.58) and a decreased free ATP/ADP ratio (from 332 normal value to 121) (Table 2). The abnormal energy state of the heart tissue can be explained by the decreased activity of respiratory complexes, including NADH: cytochrome *c* oxidoreductase and cytochrome oxidase (Table 3), and surely contributed to the development of abnormal heart funtions.

Furthermore, we observed a significant increase in ROS formation and in the amount of protein carbonyl group both in skeletal and cardiac muscle (Table 5). Protein

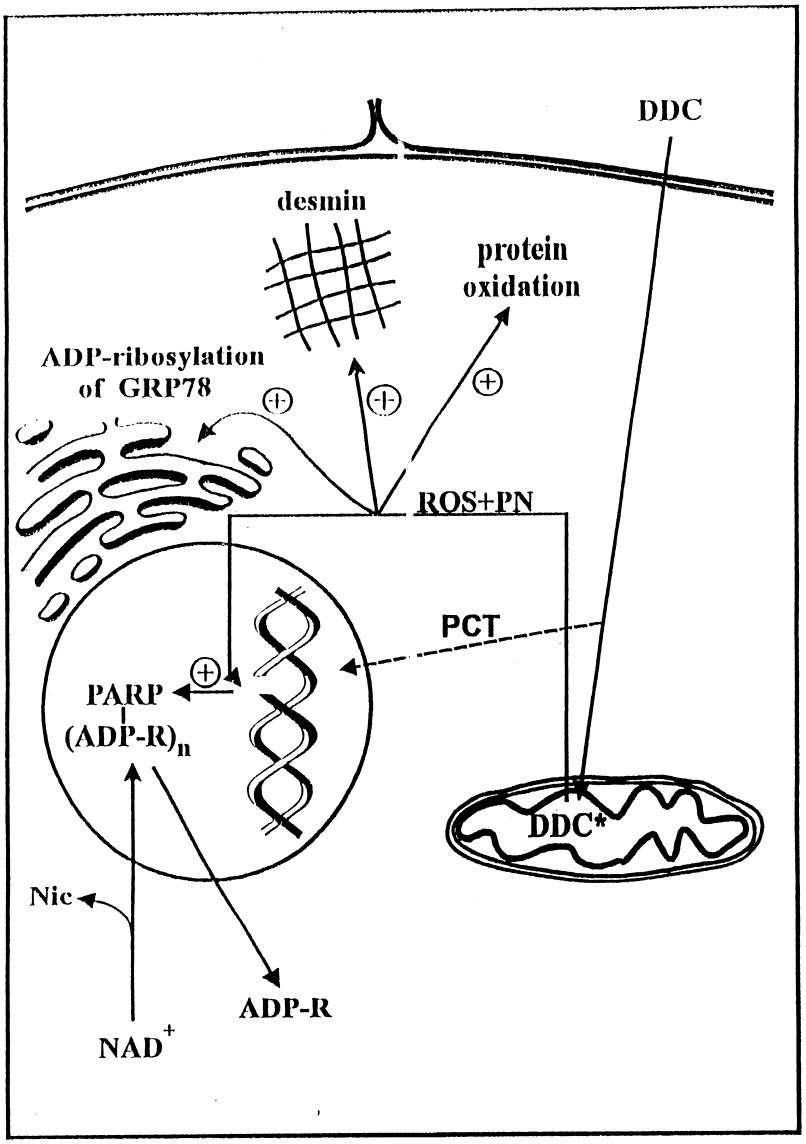

SCHEME 1. The ddC-induced signalling in rat heart. ROS, reactive oxygen species; PN, peroxynitrite; PARP, poly-ADP-ribose polymerase; Nic, nicotimamide; ADP-R, ADP-ribose; DDC, 2′,3′-dideoxycytidine; ⊕, induction or activation; PCT, premature chain termination induced by ddC-triphosphate.

carbonyl formation is considered to be a good indicator of intracellular oxidative damage [42]. The increase in ROS levels activated nuclear PARP (Fig. 3) which could cause NAD^+ depletion, and compromised energy production both in the glycolysis and citric acid cycle coupled to the respiratory chain. In addition, mono-ADP-ribosylation reactions were also induced, e.g. the ADP-ribosylation of GRP78 (Scheme 1). The GRP78 is an ER molecular chaperone which is involved in the binding of transiently nascent proteins as they are translocated into the ER [43], facilitating the attainment of the correct conformation of these proteins destined for surface expression or secretion [44]. It is well documented that ADP-ribosylation inactivates GRP78 [45] and, in turn, inhibits the folding and transport of proteins in the lumen of ER. Therefore, the induction of ADP-ribosylation of GRP78 by ddC can be the molecular mechanism by which ddC induces damage to the ER network in muscle. Furthermore, ADP-ribosylation of desmin was also induced by ddC treatment (Fig. 3C), inhibiting its own assembly and thereby the formation of intermediate filament [46]. These observations indicate that ddC treatment activated the signalling through poly- and mono-ADP-ribosylation reactions, which could diminish the energy state of cells, and negatively affected ER and intermediate filaments.

It is well known that members of the HSP70 family are involved in the transport and assembly of mitochondrial membrane proteins, including respiratory complexes [47, 48]. Earlier, we reported a decreased level of HSP72 and HSP73 in tissues of the gastrointestinal tract [49] as a result of ddC treatment. In this work, we found a similar decrease in the level of HSP72 and HSP73 in cardiac and skeletal muscle that can affect respiratory complexes. The significant decrease in the activity of respiratory complexes (Table 3) without major changes in the polypeptide composition suggests that an impaired transport and assembly, and not protein synthesis, may be responsible for the decreased activity.

There were visible signs of change in the protein composition of skeletal muscle, and at least three different proteins were present at significantly lower concentrations in skeletal muscle of ddC-treated rats (Fig. 4). We demonstrated by sequencing the N-terminal region that the missing 16 kD protein was myoglobin. Since N-terminal sequencing failed to identify the other proteins, we used mass spectrometric methods to identify these proteins. With tandem mass spectrometry sequencing, the missing 26 kD protein was identified as triosephosphate isomerase. Since myoglobin is involved in O_2 transport and the triosephosphate isomerase is a glycolytic enzyme, these changes can affect both aerob and anaerob energy production in skeletal muscle. It is known that expression of glycolytic enzymes is controlled by hypoxia-inducible factor-1α [50, 51], and an increased ROS level inactivates hypoxia-inducible factor-1α [52]. In addition, myoglobin [53] and HSP72 [54] levels are increased by hypoxia, which in turn is associated with low ROS levels. However, expression of HSP72 is activated by H_2O_2 [55], although probably by a different mechanism, indicating that increased ROS levels alone cannot explain the changes in the expression of these proteins.

From the data of this work, we conclude that prior to damaging the mitochondrial genome, ddC treatment influences cellular metabolism and signal transduction at several points. First, by increasing ROS levels it causes non-specific protein and membrane damage. Second, the increased ROS level activates poly- and mono-ADP-ribose transferases, leading to enhanced ADP-ribosylation of proteins including GRP78, desmin, and PARP in heart muscle (Scheme 1). The decreased level of HSP70s and deceased activity of the mono-ADP-ribosylated proteins cause a malfunction in protein folding and transport in the ER lumen, in intermediate filament formation, and in mitochondrial protein assembly, leading to an impaired energy supply. Finally, in skeletal muscle, the decrease in myoglobin and triosephosphate isomerase levels further impairs energy metabolism. In summary, these processes constitute a new mtDNA-independent mechanism by which ddC-induced cell damage contributes to the development of cardiomyopathy.

We thank Bertalan Horvath and Laszlo Giran for their excellent technical help. This work was supported by the Hungarian Science Foundation (OTKA Grants T020622, T26624, and T023076), the Ministry of Health and Welfare (Grant ETT 382/96), the Ministry of Education (Grant FKFP 1393/1997), and the Phare-Accord Programme (Grant H9112-434).

References

1. Copeland WC, Cheng MS and Wang TSF, Human DNA polymerase are able to incorporate anti-HIV deoxynucleotides into DNA. *J Biol Chem* **267:** 21459–21464, 1992.
2. Meng TC, Fischl MA, Boota AM, Spector SA, Bennett D, Bassiakos Y, Lai SH, Wright B and Richman DD, Combination therapy with zidovudine and dideoxycytidine in patients with advanced human immunodeficiency virus infection: A phase I/II study. *Ann Intern Med* **116:** 13–20, 1992.
3. Lipsky JJ, Zalcitabine and didanosine. *Lancet* **341:** 30–32, 1993.
4. von der Helm K, Retroviral proteases: Structure, function and inhibition from a non-anticipated viral enzyme to the target of a most promising HIV therapy. *Biol Chem* **377:** 765–774, 1996.
5. Deminie CA, Bechtold CM, Stock D, Alam M, Djang F, Balch AH, Chou TC, Prichard M, Colonno RJ and Lin PF, Evaluation of reverse transcriptase and protease inhibitors in two-drug combinations against human immunodeficiency virus replication. *Antimicrob Agents Chemother* **40:** 1346–1351, 1996.
6. Indorf AM and Pegram PS, Esophageal ulceration related to zalcitabine(ddC). *Ann Intern Med* **117:** 133–134, 1992.
7. Lerza R, Castello G, Mela GS, Arboscello E, Cerruti A, Bogliolo G, Mencoboni M, Ballarino P and Pannacciulli I, *In vitro* synergistic inhibition of human bone marrow hemopoetic progenitor growth by a 3′-azido-3′-deoxy-thymidine, 2′,3′-dideoxycytidine combination. *Exp Hematol* **25:** 252–255, 1997.
8. Izuta S, Saneyoshi M, Sakurai T, Suzuki M, Kojima K and Yoshida S, The 5′-triphosphates of 3′-azido-3′-deoxythymidine and 2′,3′-dideoxynucleosides inhibit DNA polymerase gamma by different mechanisms. *Biochem Biophys Res Commun* **179:** 776–783, 1991.
9. Chen CH, Vazquez-Padua M and Cheng YC, Effect of anti-human immunodeficiency virus nucleoside analogs on mitochondrial DNA and its implication for delayed toxicity. *Mol Pharmacol* **39:** 625–628, 1991.
10. Chen CH and Cheng JC, Delayed cytotoxicity and selective loss of mitochondrial DNA in cells treated with the anti-human immunodeficiency virus compound 2′,3′-dideoxycytidine. *J Biol Chem* **264:** 11934–11937, 1989.
11. Lewis LD, Hamzeh FM and Lietman PS, Ultrastructural changes associated with reduced mitochondrial DNA and impaired mitochondrial function in the presence of 2′,3′-dideoxycytidine. *Antimicrob Agents Chemother* **36:** 2061–2065, 1992.
12. Herskowitz A, Willoughby SB, Baughman KL, Schulman SP and Bartlett JD, Cardiomyopathy associated with antiretroviral therapy in patients with HIV infection. *Ann Intern Med* **116:** 311–313, 1992.
13. Simpson DM and Wolfe DE, Neuromuscular complications of HIV infection and its treatment. *AIDS* **5:** 917–926, 1991.
14. Yarchoan R, Perno CF, Thomas RV, Klecker RW, Allain JP, Wills RJ, McAtee N, Fischl MA, Dubinsky R and McNeely MC, Phase I studies of 2′,3′-dideoxycytidine in severe human immunodeficiency virus infection as a single agent and alternating with zidovudine(AZT). *Lancet* **11:** 76–8, 1988.
15. Chen CH and Cheng YC, The role of cytoplasmic deoxycytidine kinase in the mitochondrial effects of the anti-human immunodeficiency virus compound, 2′,3′-dideoxycytidine. *J Biol Chem* **267:** 2856–2859, 1992.
16. Benbrik E, Chariot P, Bonavaud S, Ammi-Said M, Frisdal E, Rey C, Gherardi R and Barlovatz-Meimon G, Cellular and mitochondrial toxicity of zidovudine (AZT), didanosine (ddI) and zalcitabine (ddC) on cultured human muscle cells. *J Neurol Sci* **149:** 19–25, 1997.
17. Blum AS, Dal-Pan GJ, Feinberg J, Raines C, Mayjo K, Cornblath DR and McArthur JC, Low-dose zalcitabine-related toxic neuropathy: Frequency, natural history, and risk factors. *Neurology* **46:** 999–1003, 1996.
18. MacFarlene PW and Lawrie TDV, *Comprehensive Electrocardiology*. Pergamon, Oxford, 1989.
19. Sumegi B, Gilbert HF and Srere PA, Interaction between citrate synthase and thiolase. *J Biol Chem* **260:** 188–190, 1985.
20. Sumegi B, Melegh B, Adamovich K and Trombitas K, Cytochrome oxidase deficiency affecting the structure of the

myofibre and the shape of mitochondrial cristae membrane. *Clin Chim Acta* **192:** 9–18, 1990.
21. Bergmayer HU (Ed.), *Methods in Enzymatic Analysis*, 2nd ed. Academic Press, New York, 1974.
22. Laemmli UK, Cleveage of structural proteins during the assembly of the head of bacteriophage T4. *Nature* **227:** 680–685, 1970.
23. Royall JA and Ischiropoulos H, Evaluation of 2′,7′-dichlorofluorescin and dihydrorhodamine123 as fluorescent probes for intracellular H_2O_2 in cultured endothelial cells. *Arch Biochem Biophys* **302:** 348–355, 1993.
24. Szabados E, Fischer MG, Toth K, Csete B, Nemeti B, Trombitas K, Habon T, Endrei D and Sumegi B, Role of reactive oxygen species and poly-ADP-ribose polymerase in the development of AZT-induced cardiomyopathy in rat. *Free Radic Biol Med* **26:** 309–317, 1999.
25. Patterson SD and Aebersold R, Mass spectrometric approaches for the identification of gel-separated proteins. *Electrophoresis* **16:** 1791–1814, 1995.
26. Qin J, Fenyo D, Zhao Y, Hall WW, Chao DM, Wilson CJ, Young RA and Chait BT, A strategy for rapid, high-confidence protein identification. *Anal Chem* **69:** 3995–4001, 1997.
27. Sambrook J, Fritsch EF and Maniatis T, *Molecular Cloning. Cold Spring Harbor Laboratory Press*, Cold Spring Harbor, 1989.
28. Palva TK and Palva ET, Rapid isolation of animal mitochondrial DNA. *FEBS Lett* **192:** 267–270, 1985.
29. Ohta H, Sweeney EA, Masamune A, Yatomi Y, Hakomori S and Igarashi Y, Induction of apoptosis by sphingosine in human leukemic HL-60 cells: A possible endogenous modulator of apoptotic DNA fragmentation occurring during phorbol ester-induced differentiation. *Cancer Res* **55:** 691–697, 1995.
30. Boog CJP, De Graeff-Meeder ER, Lucassen MA, van der Zee R, Voorhorst-Ogink MM, van Kooten PJ, Geuze HJ and van Eden W, Two monoclonal antibodies generated against human hsp60 show reactivity with synovial membranes of patients with juvenile chronic arthritis. *J Exp Med* **175:** 1805–1810, 1992.
31. Velez-Granell CS, Arias AE, Torres-Ruiz JA and Bendayan M, Molecular chaperones in pancreatic tissue: The presence of cnp10, cnp60 and hsp70 in distinct compartments along the secretory pathway of the acinar cells. *J Cell Sci* **107:** 539–549, 1994.
32. Oliver CN, Ahn BW, Moerman EJ, Goldstein S and Stadtman ER, Age-related changes in oxidized proteins. *J Biol Chem* **262:** 5488–5491, 1987.
33. Huang HJ, Zhou H, Huiatt TW and Graves DJ, Target proteins for arginine-specific mono(ADP-ribosyl)transferase in membrane fractions from chick skeletal muscle cells. *Exp Cell Res* **226:** 147–153, 1996.
34. Thyberg J, Hultgardh-Nilsson A and Kallin B, Inhibitors of ADP-ribosylation suppress phenotypic modulation and proliferation of smooth muscle cells cultured from rat aorta. *Differentiation* **59:** 243–252, 1995.
35. Burkle A, Chen G, Kupper JH, Grube K and Zeller WJ, Increased poly(ADP-ribosyl)ation in intact cells by cisplatin treatment. *Carcinogenesis* **14:** 559–561, 1993.
36. Piron KJ and McMahon KK, Localization and partial characterization of ADP-ribosylation products in hearts from adult and neonatal rats. *Biochem J* **270:** 591–597, 1990.
37. Tanaka Y, Yoshihara K and Kamiya T, Enzymic and nonenzymic mono ADP-ribosylation of proteins in skeletal muscle. *Biochem Biophys Res Commun* **163:** 1063–1070, 1989.
38. Leno GH and Ledford BE, ADP-ribosylation of the 78 kDa glucose-regulated protein during nutritional stress. *Eur J Biochem* **186:** 205–211, 1989.
39. Hobbs GA, Keilbaugh SA, Rief PM and Simpson MV, Cellular targets of 3′-azido-3′-deoxythymidine: An early (non-delayed) effect on oxidative phosphorylation. *Biochem Pharmacol* **50:** 381–390, 1995.
40. Modica-Napolitano JS, AZT causes tissue-specific inhibition of mitochondrial bioenergetic function. *Biochem Biophys Res Commun* **194:** 170–177, 1993.
41. Yan JP, Ilsley DD, Frohlick C, Steet R, Hall ET, Kuchta RD and Melancon P, 3′-Azidothymidine (zidovudine) inhibits glycosylation and dramatically alters glycosphingolipid synthesis in whole cells at clinically relevant concentrations. *J Biol Chem* **270:** 22836–22841, 1995.
42. Butterfield DA, Howard BJ, Yatin S, Allen KL and Carney JM, Free radical oxidation of brain proteins in accelerated senescence and its modulation by N-*tert*-butyl-alpha-phenylnitrone. *Proc Natl Acad Sci USA* **94:** 674–678, 1997.
43. Vogel JP, Misra LM and Rose MD, Loss of BiP/GRP78 function blocks translocation of secretory proteins in yeast. *J Cell Biol* **110:** 1885–1895, 1990.
44. Gething MJ and Sambrook J, Protein folding in the cell. *Nature* **355:** 33–45, 1992.
45. Ledford BE and Leno GH, ADP-ribosylation of the molecular chaperone GRP78/BiP. *Mol Cell Biochem* **138:** 141–148, 1994.
46. Huang HJ, Graves DJ, Robson RM and Huiatt TW, ADP-ribosylation of the intermediate filament protein desmin and inhibition of desmin assembly *in vitro* by muscle ribosyltransferase. *Biochem Biophys Res Commun* **197:** 570–577, 1993.
47. Martinus RD, Ryan MT, Naylor DJ, Herd SM, Hoogenraad NJ and Hoj PB, Role of chaperones in the biogenesis and maintenance of the mitochondrion. *FASEB J* **5:** 371–378, 1995.
48. Stuart RA, Cyr DM and Neupert W, Hsp70 in mitochondrial biogenesis: From chaperoning nascent polypeptide chains to facilitation of protein degradation. *Experientia* **50:** 1002–1011, 1994.
49. Csere P, Varbiro G, Sumegi B and Mozsik Gy, AIDS treatment and the shock protein level in the gastrointestinal tract. *Inflammopharmacology* **5:** 83–91, 1996.
50. Semenza GL, Jiang BH, Leung SW, Passantino R, Concordet JP, Maire P and Giallongo A, Hypoxia response elements in the aldolase A, enolase 1, and lactate dehydrogenase A gene promoters contain essential binding sites for hypoxia-inducible factor 1. *J Biol Chem* **271:** 32529–32537, 1996.
51. Semenza GL, Roth PH, Fang HM and Wang GL, Transcriptional regulation of genes encoding glycolytic enzymes by hypoxia-inducible factor 1. *J Biol Chem* **269:** 23757–23763, 1994.
52. Salceda S and Caro J, Hypoxia-inducible factor 1alpha (HIF-1alpha) protein is rapidly degraded by the ubiquitin-proteasome system under normoxic conditions. Its stabilization by hypoxia depends on redox-induced changes. *J Biol Chem* **272:** 22642–22647, 1997.
53. Guiang SF 3d, Widness JA, Flanagan KB, Schmidt RL, Radmer WJ and Georgieff MK, The relationship between fetal arterial oxygen saturation and heart and skeletal muscle myoglobin concentrations in the ovine fetus. *J Dev Physiol* **19:** 99–104, 1993.
54. Nakano M, Mann DL and Knowlton AA, Blocking the endogenous increase in HSP72 increases susceptibility to hypoxia and reoxygenation in isolated adult feline cardiocytes. *Circulation* **95:** 1523–1531, 1997.
55. Heufelder AE, Wenzel BE and Bahn RS, Methimazole and propylthiouracil inhibit the oxygen free radical-induced expression of a 72 kilodalton heat shock protein in Graves' retroocular fibroblasts. *J Clin Endocrinol Metab* **74:** 737–742, 1992.